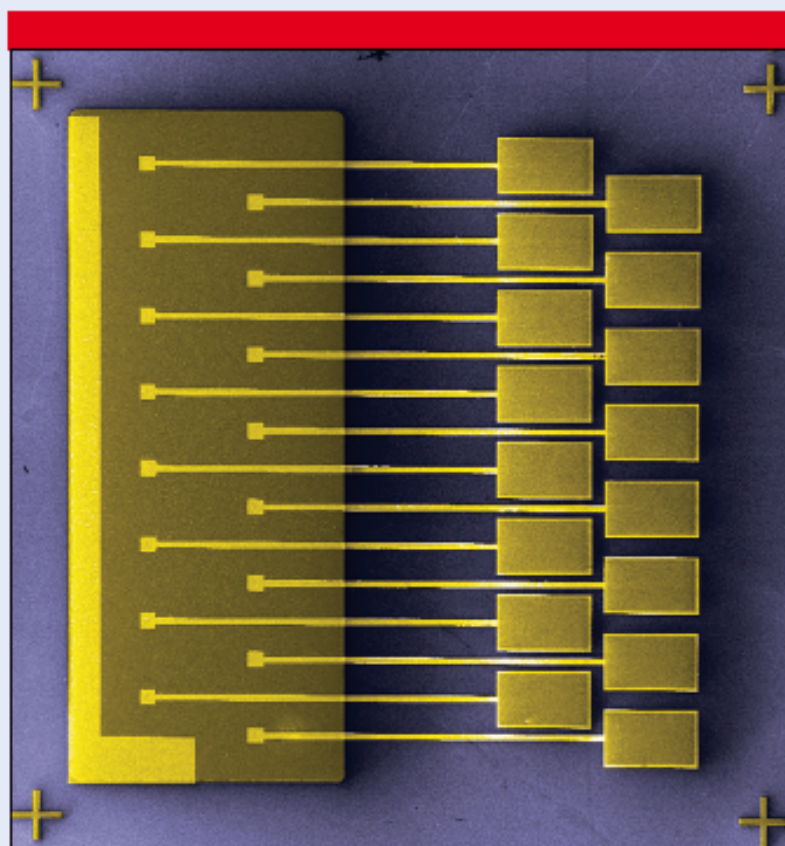


# NANOTECHNOLOGY

VOLUME 26 NUMBER 2 16 JANUARY 2015

Nanotechnology

Vol 26, No 2 020501-025702



[iopscience.org/nano](http://iopscience.org/nano)

**Featured article**

A new approach for high-yield metal–molecule–metal junctions by direct metal transfer method

*H Jeong, D Kim, P Kim, M R Cho, W-T Hwang, Y Jang, K Cho, M Min, D Xiang, Y D Park, H Jeong and T Lee*

**IOP Publishing**

16 January 2015

# A new approach for high-yield metal–molecule–metal junctions by direct metal transfer method

Hyunhak Jeong<sup>1</sup>, Dongku Kim<sup>1</sup>, Pilkwang Kim<sup>1</sup>, Myung Rae Cho<sup>1</sup>, Wang-Taek Hwang<sup>1</sup>, Yeonsik Jang<sup>1</sup>, Kyungjune Cho<sup>1</sup>, Misook Min<sup>1</sup>, Dong Xiang<sup>2</sup>, Yun Daniel Park<sup>1</sup>, Heejun Jeong<sup>3</sup> and Takhee Lee<sup>1</sup>

<sup>1</sup>Department of Physics and Astronomy, Institute of Applied Physics, Seoul National University, Seoul 151-747, Korea

<sup>2</sup>School of Mathematics and Physics, China University of Geosciences, Wuhan 430074, People's Republic of China

<sup>3</sup>Department of Applied Physics, Hanyang University, Ansan 426-791, Korea

E-mail: [hjeong@hanyang.ac.kr](mailto:hjeong@hanyang.ac.kr) and [tlee@snu.ac.kr](mailto:tlee@snu.ac.kr)

Received 12 July 2014, revised 15 October 2014

Accepted for publication 17 November 2014

Published 16 December 2014



CrossMark

## Abstract

The realization of high-yield, stable molecular junctions has been a long-standing challenge in the field of molecular electronics research, and it is an essential prerequisite for characterizing and understanding the charge transport properties of molecular junctions prior to their device applications. Here, we introduce a new approach for obtaining high-yield, vertically structured metal–molecule–metal junctions in which the top metal electrodes are formed on alkanethiolate self-assembled monolayers by a direct metal transfer method without the use of any additional protecting interlayers in the junctions. The fabricated alkanethiolate molecular devices exhibited considerably improved device yields ( $\sim 70\%$ ) in comparison to the typical low device yields (less than a few %) of molecular junctions in which the top metal electrodes are fabricated using the conventional evaporation method. We compared our method with other molecular device fabrication methods in terms of charge transport parameters. This study suggests a potential new device platform for realizing robust, high-yield molecular junctions and investigating the electronic properties of devices.

 Online supplementary data available from [stacks.iop.org/NANO/26/025601/mmedia](http://stacks.iop.org/NANO/26/025601/mmedia)

Keywords: molecular electronics, self-assembled monolayer, metal–molecule–metal junction, alkanethiolates, direct metal transfer

(Some figures may appear in colour only in the online journal)

## 1. Introduction

The field of molecular electronics, which utilizes molecules as an electronic device component, has recently received considerable attention as a potential alternative for silicon-based electronics [1–10]. To investigate the mechanism and characteristics of charge transport through molecular junctions, a variety of approaches for constructing molecular junctions, such as mechanically controllable break junction techniques, scanning probe microscopy-based techniques, and solid-state

device-based methods, have been demonstrated [3, 5–6, 10–24]. Specifically, the simple vertically structured, solid-state device-based metal–molecule–metal junctions were considered to be a general testbed for studying the charge transport characteristics of molecular junctions and their device applications [11, 15, 17, 19, 22–23]. However, one of the typical obstacles that may be encountered when forming molecular junctions using this method is that conducting filamentary paths may be formed through the molecules by the metal electrode evaporated on the molecular layers, which

results in a very low device yield of molecular junctions and renders them inappropriate as a reliable testbed platform of molecular junctions [14–15, 25–29]. To overcome this obstacle, methods that utilize an intermediate protecting layer between the molecular layer and the top electrode have been reported. For example, a conducting polymer of poly(3,4-ethylenedioxythiophene) polystyrene sulfonate (known as PEDOT:PSS), graphene, and reduced graphene oxide (rGO) have been adopted as the interlayer to improve the device yield of molecular junctions by prohibiting the formation of conducting filamentary paths [11, 19, 22, 30–33, 60, 61]. Despite this improvement, these methods also have some drawbacks: (1) the device fabrication procedure may be more complicated because of the introduction of an additional interlayer, (2) the molecular layer can be damaged or contaminated by the additional interlayer, (3) the interlayer limits the potential choices of top electrodes that can enrich the functionality of molecular junctions through interactions between the molecular layer and top electrode, (4) the formation of symmetric molecular junctions is generally impossible, and (5) the junction conductivity is relatively poor compared to metal–molecule–metal junctions without interlayers. For these reasons, pure metal–molecule–metal junctions without any additional interlayers are generally more desirable.

In this study, we propose a new approach for creating high-yield molecular devices as a vertical metal–molecule–metal junction. We fabricated the top metal electrodes using a direct metal transfer (DMT) method in which the top electrodes are formed on a different substrate and then transferred to the molecular junctions, similar to the well-known graphene transfer method [34–36]. Using this method, we were able to fabricate highly stable and reliable metal–molecule–metal junctions without the use of any additional interlayers, and the resulting junctions exhibited considerably improved device yields ( $\sim 70\%$ ) compared to those (typically less than a few %) of the molecular junctions in which the top electrodes are formed using the conventional metal-evaporation method [15, 37]. We compared this method with other molecular device fabrication methods in terms of characteristic charge transport parameters, especially the electronic coupling interaction between the molecular layer and electrodes. Also we summarized the strengths and weaknesses of our method in comparison with other methods.

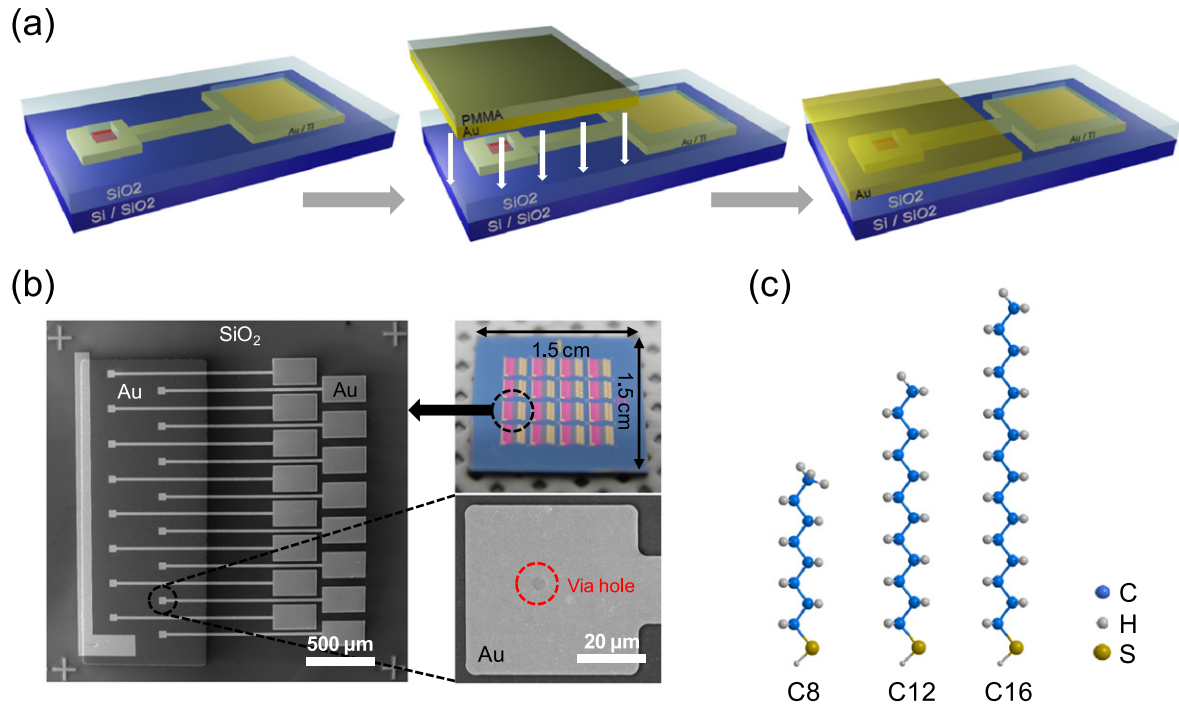
## 2. Experimental details

Figure 1(a) presents a schematic illustration of the process for fabricating the molecular junctions using the DMT method. In this study, we selected alkanethiolate ( $\text{HS}(\text{CH}_2)_{n-1}\text{CH}_3$ ) self-assembled monolayers (SAMs) for the molecular junctions because alkanethiolates, which have a structure composed of repetitively connected alkyl chains with thiol end groups, are one of the most widely studied molecules for use in a variety of junction fabrication techniques. Many research groups have reported the charge transport properties of alkanethiolates in molecular junctions based on the use of various

techniques, such as scanning tunneling microscopy [24], mechanically controllable break junction [10, 38, 63], conducting-probe atomic force microscopy [39], nanopores [23], electromigration nanogap [20, 40] and solid-state device testbeds [11, 15, 19, 22]. Therefore, the alkanethiolates can be considered as reference molecules for evaluating the characteristics of the newly proposed molecular junction testbeds. Here, we used three different lengths of alkanethiolate molecules: octanethiol ( $\text{HS}(\text{CH}_2)_7\text{CH}_3$ , denoted as C8), dodecanethiol ( $\text{HS}(\text{CH}_2)_{11}\text{CH}_3$ , denoted as C12), and hexadecanethiol ( $\text{HS}(\text{CH}_2)_{15}\text{CH}_3$ , denoted as C16). The reasons for choosing these three molecules are because (1) sufficient difference in alkane lengths is necessary for definite distinction in electrical properties especially current density. This definite distinction of current density enables the statistical analysis to be quite distinguishable, and (2) similar alkane lengths of molecules should be chosen as previous works for proper comparison of each method [11, 22, 32, 58–60]. The chemical structures of these molecules are presented in figure 1(c).

To form the molecular junctions, we employed a fabrication procedure that was previously reported by our group [15, 19, 22]. Briefly, conventional optical lithography was first used to pattern the bottom electrodes on Si/SiO<sub>2</sub> substrates. After the evaporation of the bottom electrodes (50 nm thick Au/5 nm thick Ti), the residual photoresist was removed using the lift-off technique, and the SiO<sub>2</sub> insulating walls were generated by plasma-enhanced chemical vapor deposition. Then, circular holes with radii of 2, 3, 4, and 5  $\mu\text{m}$  were created on the insulating wall through optical lithography to expose the Au top surface which is used as bottom electrodes. Because the bottom gold electrode is the top surface of the evaporated gold, it is necessary to investigate roughness of the gold surfaces for the molecular junction. For this, we have included surface morphology image of the bottom gold electrodes, obtained with an atomic force microscope in the supplementary data (figure S2). Alkanethiolate SAMs were formed on the exposed Au surfaces by immersing the substrates in an ethanolic solution of alkanethiolate molecules. After the alkanethiolates were self-assembled on the Au surface, the top electrodes were generated. Generally, when one creates vertical metal–molecule–metal junctions, the device yield is very poor (less than a few %) because of the formation of conducting filamentary paths through the molecular layer during the evaporation of the top metal electrode [14–15, 25–29]. To prevent this problem, methods for inserting an intermediate layer between the top electrode and molecular layer have been demonstrated, in which the interlayer acts as the electrode to contact molecules and as the blocking layer for the Au top electrode [11, 19, 22, 30–33, 60, 61]. These interlayer-electrode molecular junctions exhibited considerably higher device yields, but at the same time, they may complicate the interpretation of the molecular junction's properties because of the additional interfaces resulting from the introduction of the interlayer [41].

In this study, we transferred a patterned top metal sheet as the top electrode onto the molecular layers. Figure 2 presents photographic images of the preparation procedure



**Figure 1.** (a) Schematic illustration of the molecular junction formation procedure; (1) bottom electrode and insulating wall are generated by following procedures depicted in the section 2. The small red dots represent the SAM on the Au top surface of bottom electrode. (2) The transfer film is placed on the molecular junction area. (3) The molecular junction fabrication is finished by removing residual PMMA on the transfer film. (b) SEM and optical microscopy images of the fabricated molecular devices. (c) The three types of alkanethiols along with their chemical structures: C8 (octanethiol), C12 (dodecanethiol) and C16 (hexadecanethiol).

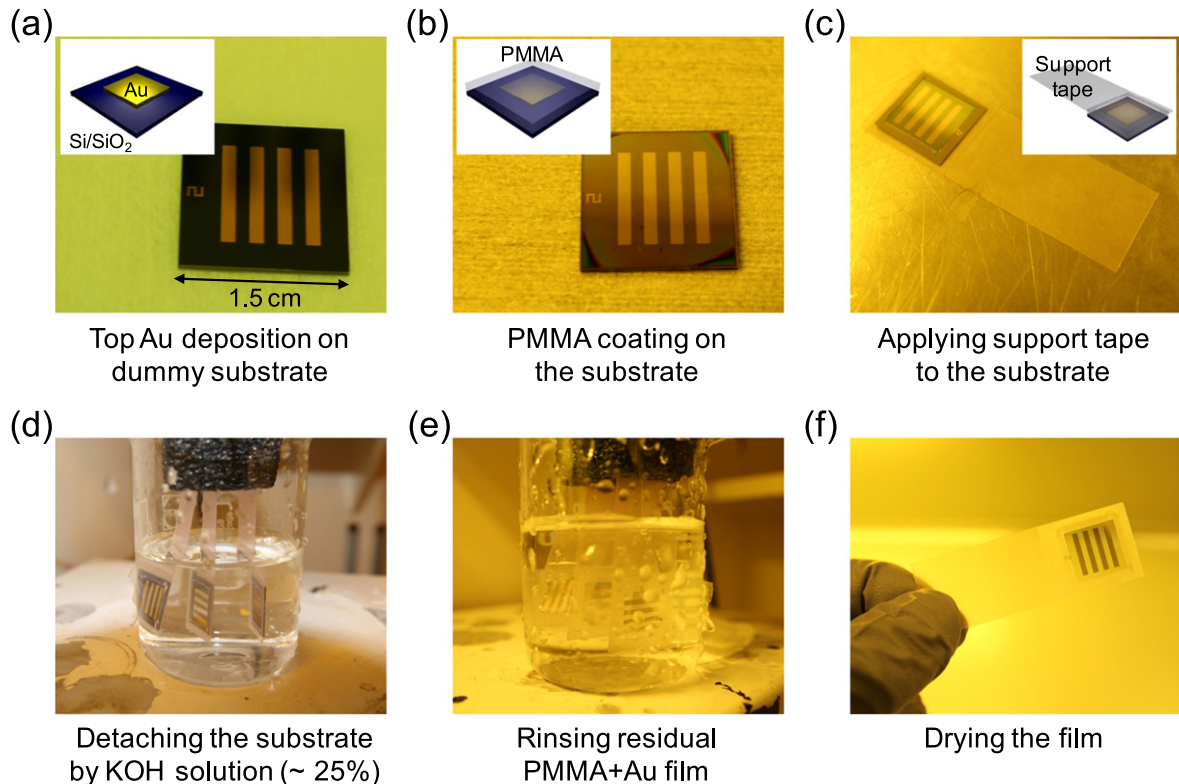


**Figure 2.** Optical and schematic images of the preparation procedure for transferring the Au film. (a) Patterned top Au electrode deposited on a dummy substrate. (b) PMMA was spin-coated on the dummy substrate. (c) A support tape was applied to support the substrate. (d) To detach the substrate, the film was immersed in a KOH solution. (e) Residual film was removed by rinsing the substrate. (f) Drying the residual film.

**Table 1.** Summary of the statistical analysis results for the molecular devices fabricated using the DMT method in this study.

Molecules	Number of fabricated devices	Fab. failure	Short	Open	Non-working	Working	Device yield
C8	128 (100.0%)	0 (0.0%)	25 (19.5%)	0 (0.0%)	1 (0.8%)	102 (79.7%)	272 (70.8%)
C12	128 (100.0%)	3 (2.3%)	14 (10.9%)	0 (0.0%)	19 (14.8%)	92 (71.9%)	
C16	128 (100.0%)	11 (8.6%)	12 (9.4%)	26 (20.3%)	1 (0.8%)	78 (60.9%)	

steps for transferring the top Au electrodes. As the first step for preparing the transfer film, we deposited the patterned top Au electrodes onto a dummy substrate (SiO<sub>2</sub>/Si) with an electron beam evaporator using a shadow mask, as shown in figure 2(a). The inset of figure 2(a) presents a schematic image of the Au electrodes on the dummy substrate. Then, poly(methyl methacrylate) (PMMA) was spin-coated onto the dummy substrate to support the Au electrodes while the film was detached from the substrate (figure 2(b)). After coating, we applied a support tape to the top of the substrate (figure 2(c)). Because the tape is used for immersing the substrate in the etching solution, we attached a dummy sample on one end of the tape. Additionally, to prevent mechanical damage to the Au electrodes while handling the film, we removed the part of the tape above the substrate. Then, the top Au electrodes with a thin PMMA layer were detached from the dummy substrate by immersing the film into a potassium hydroxide (KOH) solution (~25%) for approximately one hour. Because the SiO<sub>2</sub> layer on the substrate will be etched by this etching solution, the Au electrode can be detached. Finally, the detached transfer film was gently rinsed several times with deionized water and gently dried with a N<sub>2</sub> stream (see figures 2(e) and (f)). By applying this film on the molecular monolayer, vertical metal–molecule–metal junctions were generated. To facilitate fine contact between the Au electrodes and the molecular layer, we added a couple of drops of isopropyl alcohol (IPA) to the molecular junction substrate before making contact with the transfer PMMA film. The capillary action resulting from the surface tension of IPA during vaporization enables the transfer film to make a fine contact with the molecular layer. Also we granted very low aspect ratio i.e. isolation wall height to junction width of the maximum 1:200 (see the supplementary data). With this low aspect ratio, at least it is possible to make fine contact around the center of the junction except the edge of the isolation wall. Finally, the remaining PMMA was removed by dipping the samples in acetone. Figure 1(b) presents optical and scanning electron microscopy (SEM) images of the molecular junctions fabricated using this method. Details of the fabrication procedure are provided in the supplementary data. Through the use of this method, we were able to considerably improve the device yield (~70%) with a pure metal–molecular monolayer–metal junction structure (table 1).

### 3. Results and discussion

One of the most remarkable advantages of fabricating molecular junctions using a solid-state device structure is the capability of mass production because the fabrication can be performed using conventional manufacturing processes. Mass production provides a statistically sufficient number of molecular devices to be analyzed. Additionally, the statistical analysis enables us to distinguish the genuine transport characteristics of molecular junctions from uncertainly collected electrical information [15, 22, 29, 42]. In this study, we fabricated a statistically meaningful number of molecular junctions. Specifically, 128 molecular junctions for each C8, C12 and C16 molecule were fabricated and analyzed (a total of 384 molecular junctions). Additionally, we found that the device yields were ~70%, indicating that approximately 70% of the molecular junctions fabricated using this method exhibited molecularly determined charge transport properties (see table 1). We defined ‘molecularly working’ devices based on the previously reported statistical criteria [15] and observed that the device yield remarkably improved compared to that (less than a few %) for the same device structure of metal–molecule–metal junctions in which the top electrodes were created using conventional evaporation [15, 25, 27, 29]. For a brief explanation of the criteria, figure 3(b) presents the histograms of log<sub>10</sub> (current density (*J*)) values measured at 1.0 V for each ‘candidate’ C8, C12 and C16 molecular device. The candidate devices represent the molecular junctions that exhibit non-linear current–voltage characteristics, with the exception of obvious electrical shorts or open and fabrication failure. Then, we performed Gaussian fittings using the least squares method on the histograms using normal distribution functions,

$$f(x) = \frac{1}{\sqrt{2\pi\sigma^2}} \exp\left[-\frac{(x - \mu)^2}{2\sigma^2}\right], \quad (1)$$

where  $\mu$  is the Gaussian average, and  $\sigma$  is the Gaussian standard deviation. Finally, we limited the range of working devices such that the log<sub>10</sub> (*J*) value lies within the arbitrarily chosen  $3\sigma$  range corresponding to  $\mu - 3\sigma$  and  $\mu + 3\sigma$ . Through these criteria, we were able to select 99.7% of the working devices from the entire population of candidates and determined the device yield to be ~70%.

Figure 3(a) shows the representative current density–voltage (*J*–*V*) characteristics of the working molecular devices in this study. Here, the error bars indicate the previously

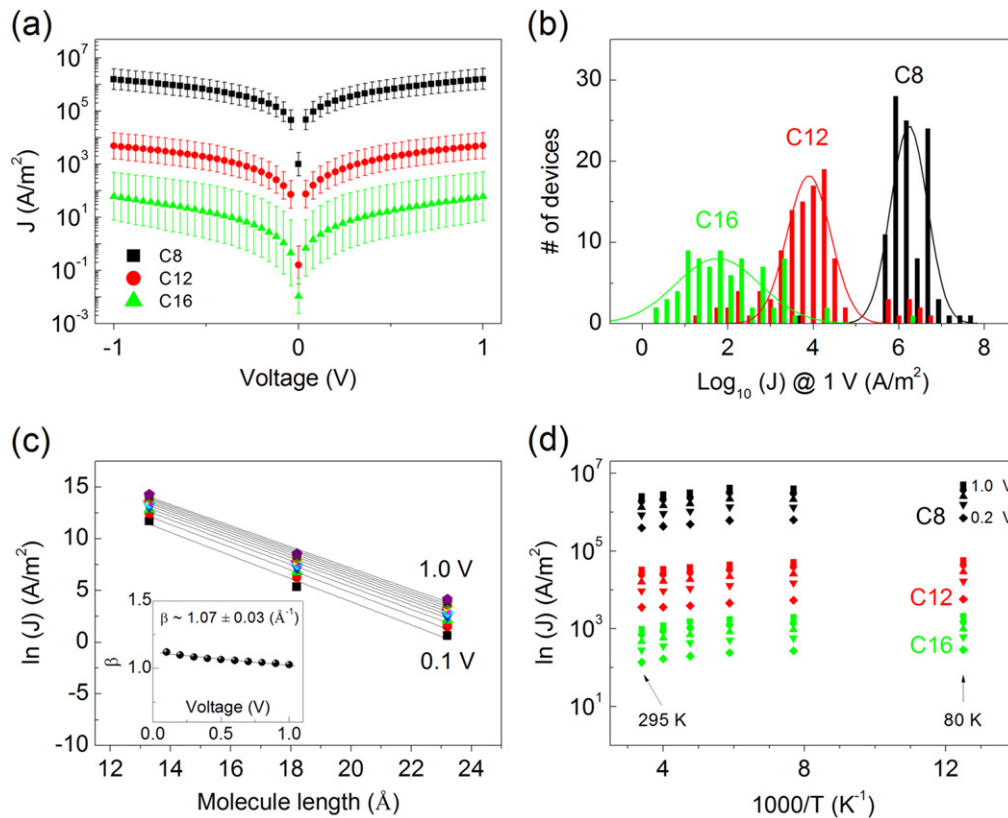


**Figure 3.** (a) Statistical  $J$ - $V$  data for all C8, C12, and C16 working devices. (b) Histogram of the logarithmic current densities at 1 V for all 'candidate' molecular devices. Solid curves represent the Gaussian fitting results. (c) A semi-log plot of the current densities measured at different biases as a function of the molecular length. Solid lines represent the exponential fitting results, in which the slope is related to the decay coefficient  $\beta$ . The inset shows the values of  $\beta$  deduced from the plot versus the applied bias. (d) Arrhenius plot of the logarithmic current densities for C8, C12 and C16 molecular devices at different biases from 0.2 V to 1.0 V in 0.2 V increments. The temperature was varied from 80 K to 295 K in 40 K increments.

obtained Gaussian standard deviations of working molecular devices. According to a number of studies, the primary conduction mechanism through alkanethiolates is known as off-resonant tunneling [15, 43–45]. Therefore, the exponential dependence of the current density on the molecular length (i.e.,  $J = J_0 \exp(-\beta d)$ , where  $\beta$  is the decay coefficient and  $d$  is the molecular length) can be evidence for the actual realization of alkanethiolate molecular junctions [11, 15, 19, 22, 29, 43–44]. We found that the current density was exponentially dependent on the molecular length, as shown in figure 3(c). Figure 3(c) displays the semi-log plot of the current densities versus the molecular length from 0.1 V to 1.0 V in increments of 0.1 V. From the magnitude of each linear fitting slope, which corresponds to the decay coefficient, we could determine  $\beta$  for each bias. The determined values of  $\beta$  for each bias are shown in the inset of figure 3(c). The average value of  $\beta$  was determined to be  $1.07 \pm 0.03 \text{ \AA}^{-1}$ , which is in agreement with many previously reported studies on alkanethiolate molecular junctions [43, 46–51]. To verify the off-resonant tunneling transport mechanism through alkanethiolates, we investigated the relationship between the current density and temperature ( $T$ ). Figure 3(d) shows the Arrhenius plots (i.e.,  $\ln(J)$  as a function of  $1/T$ ) at different biases ranging from 0.2 V to 1.0 V in increments of 0.2 V. Additionally, the temperature was changed from 80 K to

295 K in increments of 40 K. As shown in this figure, the molecular devices exhibited almost temperature-independent current density characteristics, providing direct evidence of tunneling transport properties. Through these fundamental electrical characterizations of the molecular junctions (figures 3(a)–(d)), we were able to confirm the feasibility of the proposed method as a high-yield testbed with metal–molecule–metal junctions.

From the device application perspective, not only the device yield but also the stability and durability are crucial aspects of molecular junctions [5, 52–53]. These aspects also reflect the reliability and reproducibility of the characteristics of molecular junctions. Therefore, the stability and durability should be considered one of the most important factors for verifying the validity of junction testbeds. Figure 4(a) presents the  $J$ - $V$  characteristics of C8, C12 and C16 molecular junctions. Additionally, the inset of figure 4(a) shows  $J$ - $V$  curves of a representative C12 molecular junction. In this inset, we plotted the results that were measured immediately after the device was fabricated along with the results that were re-measured after 180 days after the device was exposed to ambient atmosphere. Although the molecular junction was exposed to oxygen and water vapor, no significant degradation in the transport characteristics was observed. Figure 4(b) presents the operational stability test results, in which the

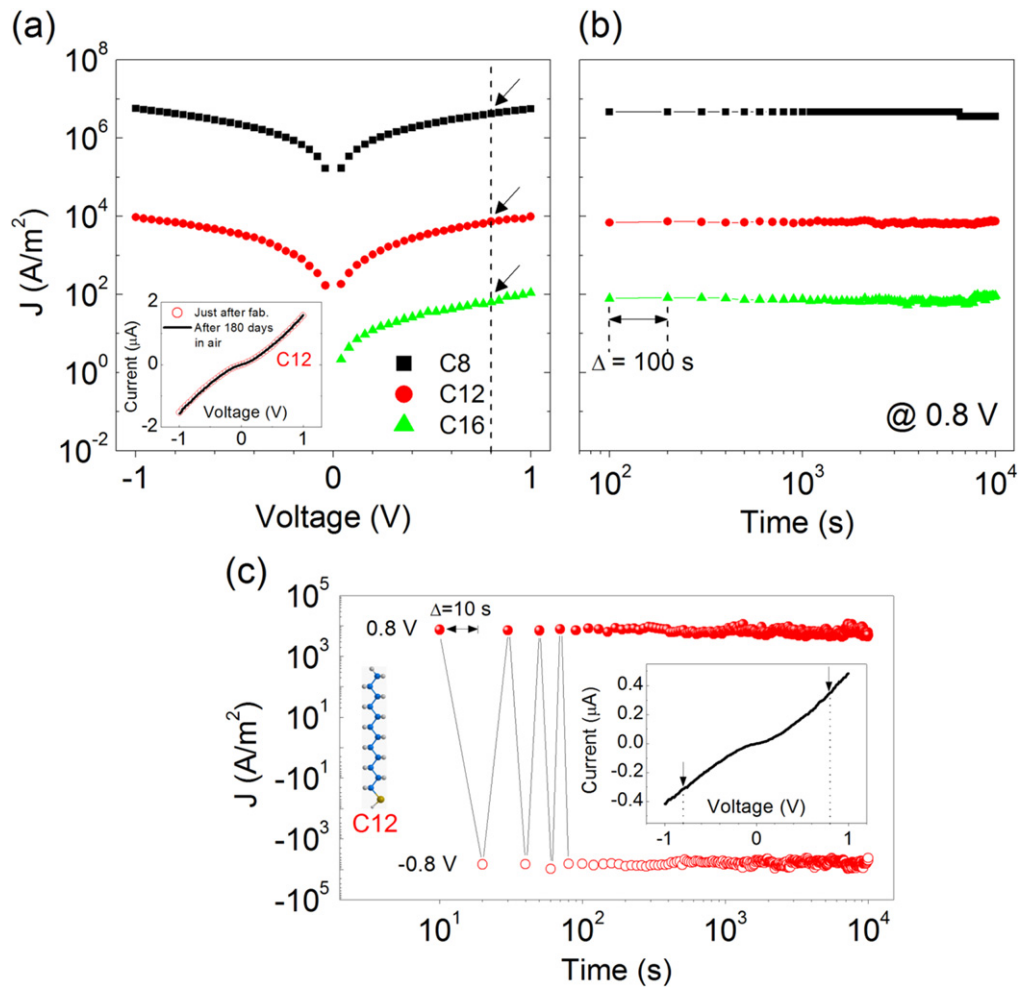


**Figure 4.** (a)  $J$ - $V$  characteristics for representative C8, C12 and C16 molecular devices. The inset shows the  $J$ - $V$  characteristics of a C12 molecular device measured immediately after fabrication (open circles) and after 180 days of exposure to ambient atmosphere (solid line). (b) Endurance characteristics of the molecular devices characterized by the current densities measured at 1.0 V for  $10^4$  s (measurement interval  $\Delta t = 100$  s). (c) Retention characteristics of a C12 molecular device. The current densities were measured at positive bias (+0.8 V) and negative bias (-0.8 V) for  $10^4$  s with an interval  $\Delta t = 10$  s.

current densities were measured at 0.8 V (black arrows in figure 4(a)) for each molecular junction as a function of time. The current density measurements were repeated every 100 s ( $\Delta t = 100$  s) until  $10^4$  s, and it was observed that the current density characteristics were well maintained without significant degradation for  $10^4$  s. Furthermore, our molecular devices exhibited good retention properties, as indicated by the results shown in figure 4(c). Even under repeated voltage stress conditions that varied from  $-0.8$  V to  $0.8$  V every 5 s for  $10^4$  s, the current densities measured at each bias did not notably change. These results reflect the excellent stability and durability of the molecular junctions fabricated using the DMT method in this study.

Now, we compare our method with other molecular device fabrication methods in terms of charge transport parameters. Among these parameters, junction conductivity (resistance) can be considered the main parameter for comparing each method. This parameter is related to the electronic coupling interaction between the molecular layer and top electrode [8, 21, 54–55]. Strong electronic coupling is

generally preferable because it can facilitate the observation of a variety of unique molecular transport properties via interactions between the molecular layer and electrode [8, 21, 54–55]. Figure 5 presents a semi-log plot of representative current densities (at a bias of  $-0.5$  V) as a function of the number of carbon bonds for alkanethiolate molecular junctions fabricated using various methods that have been previously reported to be high-yield fabrication methods (device yield > 50%; see table 2). The solid lines represent the linear fits of the current densities in the semi-log plot. The magnitude of each slope is related to the decay coefficient  $\beta$ , and the intercepts are equal to  $J_0$ , which gives to the inverse of the contact resistance. Each parameter determined from figure 5 is summarized in table 2. In figure 5, each symbol from (1) to (7) represents a molecular junction fabrication method that has been previously reported by various research groups [15, 19, 22, 32, 41, 56–58]. These fabrication methods are briefly explained in table 2. The symbol (8) represents the molecular junctions fabricated using the DMT method in this study. The estimated value of  $\beta$  from our method was

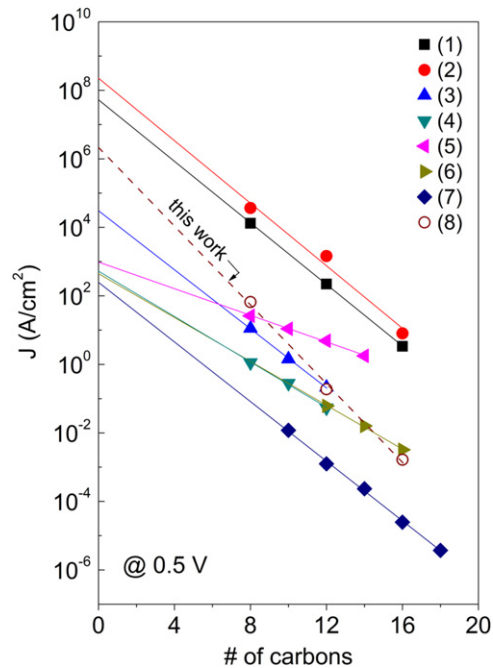


**Figure 5.** (a) A semi-log plot of the current densities at 0.5 V as a function of the number of carbon bonds for various fabrication methods. Solid lines represent the exponential fitting results, in which the slope is related to the decay coefficient  $\beta$  and the y-intercept equals  $J_0$ . The symbols represent different device fabrication methods ((1)–(8); method (8) is the method proposed in this study), and the deduced parameters and detailed descriptions for the methods are presented in table 2.

$\sim 1.07 \text{ \AA}^{-1}$ , which is slightly larger than the values from other methods but in the range of previously reported values [43, 46–51]. Comparison of this  $\beta$  value with other methods has been well established already can be an indirect and simple tool for judging whether the molecular junction is formed properly or not. In this respect, we can carefully conclude that our molecular junctions are appropriately generated by our new method. More importantly, the  $J_0$  value using our method was determined to be  $\sim 2.2 \times 10^6 \text{ A cm}^{-2}$ , which is noticeably higher than the values obtained using other methods. In particular, most of the methods that adopt an intermediate layer exhibited relatively poor values of  $J_0$  compared to our technique. This result suggests that the molecular junctions fabricated using our method possess good contact properties and strong coupling between the molecular layer and top electrodes. However, the  $J_0$  value in our method is less than that obtained in method (1) which directly evaporates the Au top electrode, mainly because of the transferring process to create top Au electrodes in our method, but method (1) typically exhibits a very low device yield (less than a few %). Here, we suppose that damage to the SAM, nonconformal contact, and defects on the top Au film resulting from physical nature of our fabrication process may lead to degradation of electrical properties of our molecular junctions (see the supplementary data). Therefore, considering all these results, our DMT method can be considered a good molecular junction platform to provide a strong and

stable electronic coupling between the top electrode and molecular layer with a high device yield.

Finally, we discuss in details the advantages and disadvantages of our method in comparison with other methods. To this end, we carefully selected five different methods which received the intensive attention of different research groups in this field and compared their advantages and disadvantages each other as summarized in table 3. Based on the comparison, our new method has several strengths compared to other methods, for example: (1) the structure of our molecular junction is familiar and comfortably conservative system because the two electrodes are made of common metals. This familiarity provides convenience in utilization that enables to reproduce the molecular junctions easily. (2) Because of the usage of the common metals for the electrodes, the molecular junctions can be diversified simply by choosing the kind of metals to one's preference. Generally, it is known that various common metals have peculiar effects on molecules such as different energy band alignment, packing density, and magnetic effects. Therefore by choosing various kinds of metal electrodes for molecular junctions, we can also diversify the functionality of molecular junctions. (3) The capability of mass production with high-yield junctions enables us to distinguish the genuine transport characteristics of molecular junctions from uncertainly collected electrical information. Because of its very small size of molecules, generally it is very difficult to generate the perfectly same molecular junctions among each fabrication. This brings variation in experimental data among each molecular junction that makes it hard to investigate the genuine properties of molecular junctions. Therefore, statistical analysis being available by the mass production of molecular junctions makes it possible to overcome this problem. Together with these advantages, however, there are limits to our method. (1) Because of its physical nature of establishing the top electrode contact with the SAM, it might not be possible to achieve ideal conformal contact. While preparing thin gold film, there were several physical processes which can bring defects on the surface of the thin gold film such as etching, rinsing, drying the film that will eventually damage the SAM (see the supplementary data). This damage and irregular contact can result in unexpected errors in the experimental data. (2) The electrical data of our molecular junctions show relatively large dispersion which implies the molecular junction lacks homogeneity. We suspect that this large dispersion originates from the physical nature of our fabrication process which results in damage to the SAM and irregular contact properties as mentioned above. Also, the dispersion can be influenced by roughness of gold surface of bottom electrode. (3) Our fabrication method is not trivial and demands a hard effort to produce the molecular junctions because the fabrication process should be handled carefully. Therefore, this method may not be suitable for practical applications of molecular electronic devices. Based on these strengths and weaknesses, there are some cases where these junctions can be applicable, for example, (1) when the statistical analysis should be applied to distinguish the genuine transport characteristics of molecular junctions especially with metal–SAM–metal

**Table 2.** Comparison of the experimental data between the DMT method of this study with other previously reported molecular device fabrication methods.

Method #	Type of junction	Technique	$\beta$ ( $\text{\AA}^{-1}$ )	$\sim J_0$ at 0.5 V ( $\text{A cm}^{-2}$ )	Yield (%)	Refs.
(1) ■	Au-SAMs/Au	Evaporated Au/micropore	0.81–0.86	$5.2 \times 10^7$	1.2–1.75	15
(2) ●	Au-SAMs/graphene-Au	Graphene/micropore	0.85	$2.3 \times 10^8$	90	22
(3) ▲	Au-SAMs/rGO-Au	Solution-processed rGO	0.82	$3.0 \times 10^4$	>99	32
(4) ▼	Au-SAMs/polymer-Au	PEDOT:PSS/micropore	0.61	$5.2 \times 10^2$	58	19, 41
(5) ◆	Au-SAMs/polymer-Au	Aedotron P/nanopore	0.44	$9.4 \times 10^2$	70–100	57
(6) ►	Au-SAMs/Au	Wedging transfer	0.58	$4.4 \times 10^2$	38–50	56
(7) ◆	Ag-SAMs/GaO <sub>x</sub> -EGaIn	Thorough-hole	0.80	$2.5 \times 10^2$	78	58
(8) ○	Au-SAMs/Au	Direct metal Transfer	1.07	$2.2 \times 10^6$	71	This work

**Table 3.** Comparison of the strengths and weaknesses between our method with other methods.

Type of junction	Advantages	Disadvantages	Ref.
Au-SAMs/Au (evaporated)	<ul style="list-style-type: none"> <li>• Relatively good contact</li> <li>• Various choice of top electrodes</li> <li>• Capability of mass production</li> <li>• Relatively easy fabrication</li> <li>• Low dependency of manufacturers</li> <li>• Low contact resistance</li> <li>• Nonvolatile, nontoxic</li> </ul>	<ul style="list-style-type: none"> <li>• Very low yield (~1–2%)</li> <li>• Physical damage to the SAM</li> <li>• High dispersion in data</li> <li>• Waste of metals</li> </ul>	15
Au-SAMs/grapheme-Au	<ul style="list-style-type: none"> <li>• High yield (~80–100%)</li> <li>• Very stable over long period</li> <li>• Capacity of mass production</li> <li>• Low contact resistance</li> <li>• Nonvolatile, nontoxic</li> </ul>	<ul style="list-style-type: none"> <li>• Physical contact of graphene (defects, damage to the SAM)</li> <li>• High dispersion in data</li> <li>• High dependency of manufacturers</li> <li>• Restriction on choice of the top electrode</li> <li>• Fabrication is relatively difficult for practical applications</li> </ul>	22
Au-SAMs/PEDOT:PSS-Au	<ul style="list-style-type: none"> <li>• High yield (~100%)</li> <li>• Very stable over long period</li> <li>• Capability of mass production</li> <li>• Relatively easy fabrication</li> <li>• High reproducibility</li> </ul>	<ul style="list-style-type: none"> <li>• Physical contact of polymer (defects, damage to the SAM)</li> <li>• Ambiguous interface between top contact</li> <li>• Restriction on choice of the top electrode</li> </ul>	11
Si-SAMs/Hg	<ul style="list-style-type: none"> <li>• Relatively good contact</li> <li>• High reproducibility</li> </ul>	<ul style="list-style-type: none"> <li>• Restriction on choice of the top electrode</li> <li>• Damage to the SAM and bottom electrode</li> <li>• Low stability in time</li> <li>• Hg is toxic and volatile.</li> <li>• Relatively low yield (~25%)</li> </ul>	62

Table 3. (Continued.)

Type of junction	Advantages	Disadvantages	Ref.
Ag-SAMs/GaO <sub>x</sub> -EGaIn	<ul style="list-style-type: none"> <li>• High yield (~80-100%)</li> <li>• Nonvolatile, nontoxic</li> <li>• High reproducibility</li> <li>• Relatively good contact</li> <li>• Low damage to the SAM and bottom electrode</li> </ul>	<ul style="list-style-type: none"> <li>• Restriction on choice of the top electrode</li> <li>• Ambiguous interface between top contact</li> <li>• Relatively low stability for practical applications</li> </ul>	58
Au-SAMs/Au (this work)	<ul style="list-style-type: none"> <li>• Relatively high yield (~70%)</li> <li>• Nonvolatile, nontoxic</li> <li>• Various choice of top electrodes</li> <li>• Capability of mass production</li> <li>• Stable over long period</li> </ul>	<ul style="list-style-type: none"> <li>• Physical contact of the top electrode (defects, damage to the SAM)</li> <li>• High dependency of manufacturers</li> <li>• High dispersion in data</li> <li>• Fabrication is relatively difficult for practical applications</li> </ul>	This work

structure from uncertainly collected electrical information, and (2) when the various choices of metal electrodes that have different contact properties with the SAM should be utilized to enrich the functionalities of molecular junctions. These cases are commonly necessary to investigate the intrinsic properties of molecules from the scientific point of view.

#### 4. Conclusion

In summary, we have demonstrated a new technique for fabricating high-yield molecular junctions in a vertical metal–molecule–metal structure in which the top metal electrodes are formed on alkanethiolate molecules using a DMT method. The molecular junctions fabricated using this method exhibited the well-known tunneling transport characteristics of alkanethiolates with good stability, durability, and device lifetime properties, which are important factors for the practical application of molecular devices. Based on the comparison of our method with other previously reported molecular device fabrication methods, our method appears to provide stronger and more stable electronic coupling between the top electrode and molecular layer, resulting in better contact properties. Our new approach may be a probable way to achieve a reliable platform for the precise characterization and practical application of molecular electronic junctions.

#### Acknowledgments

The authors appreciate the financial support from the National Creative Research Laboratory program (Grant No. 2012026372) and from the National Core Research Center program (Grant No. R15-2008-006-03002-0) through the National Research Foundation of Korea (NRF) funded by the Korean Ministry of Science, ICT and Future Planning. MRC and YDP were supported by the NRF (2014-023563, 2008-

0061906). We also appreciate Inter-university Semiconductor Research Center (ISRC) of Seoul National University.

#### References

- [1] Aviram A and Ratner M A 1974 *Chem. Phys. Lett.* **29** 277
- [2] Behin-Aein B, Datta D, Salahuddin S and Datta S 2010 *Nat. Nanotechnology* **5** 266
- [3] Chen J, Reed M A, Rawlett A M and Tour J M 1999 *Science* **286** 1550
- [4] Galperin M, Ratner M A, Nitzan A and Troisi A 2008 *Science* **319** 1056
- [5] Green J E *et al* 2007 *Nature* **445** 414
- [6] Lafferentz L, Ample F, Yu H, Hecht S, Joachim C and Grill L 2009 *Science* **323** 1193
- [7] Love J C, Estroff L A, Kriebel J K, Nuzzo R G and Whitesides G M 2005 *Chem. Rev.* **105** 1103
- [8] Moth-Poulsen K and Bjornholm T 2009 *Nat. Nanotechnology* **4** 551
- [9] Nitzan A and Ratner M A 2003 *Science* **300** 1384
- [10] Reed M A, Zhou C, Muller C J, Burgin T P and Tour J M 1997 *Science* **278** 252
- [11] Akkerman H B, Blom P W M, de Leeuw D M and de Boer B 2006 *Nature* **441** 69
- [12] Chen X, Yeganeh S, Qin L, Li S, Xue C, Braunschweig A B, Schatz G C, Ratner M A and Mirkin C A 2009 *Nano Lett.* **9** 3974
- [13] Choi S H, Kim B and Frisbie C D 2008 *Science* **320** 1482
- [14] Haick H and Cahen D 2008 *Acc. Chem. Res.* **41** 359
- [15] Kim T-W, Wang G, Lee H and Lee T 2007 *Nanotechnology* **18** 315204
- [16] Liang W J, Shores M P, Bockrath M, Long J R and Park H 2002 *Nature* **417** 725
- [17] Loo Y L, Lang D V, Rogers J A and Hsu J W P 2003 *Nano Lett.* **3** 913
- [18] Park J *et al* 2002 *Nature* **417** 722
- [19] Park S, Wang G, Cho B, Kim Y, Song S, Ji Y, Yoon M-H and Lee T 2012 *Nat. Nanotechnology* **7** 438
- [20] Song H, Kim Y, Jang Y H, Jeong H, Reed M A and Lee T 2009 *Nature* **462** 1039
- [21] Venkataraman L, Klare J E, Nuckolls C, Hybertsen M S and Steigerwald M L 2006 *Nature* **442** 904

- [22] Wang G, Kim Y, Choe M, Kim T-W and Lee T 2011 *Adv. Mater.* **23** 755
- [23] Wang W Y, Lee T, Kretzschmar I and Reed M A 2004 *Nano Lett.* **4** 643
- [24] Xu B Q and Tao N J J 2003 *Science* **301** 1221
- [25] de Boer B, Frank M M, Chabal Y J, Jiang W R, Garfunkel E and Bao Z 2004 *Langmuir* **20** 1539
- [26] Fisher G L et al 2002 *J. Am. Chem. Soc.* **124** 5528
- [27] Haick H, Niitsoo O, Ghabboun J and Cahen D 2007 *J. Phys. Chem. C* **111** 2318
- [28] Walker A V, Tighe T B, Cabarcos O M, Reinard M D, Haynie B C, Uppili S, Winograd N and Allara D L 2004 *J. Am. Chem. Soc.* **126** 3954
- [29] Wang G, Kim T-W, Lee H and Lee T 2007 *Phys. Rev. B* **76** 205320
- [30] Jeong H et al 2014 *Adv. Funct. Mater.* **24** 2472
- [31] Min M, Seo S, Lee S M and Lee H 2013 *Adv. Mater.* **25** 7045
- [32] Seo S, Min M, Lee J, Lee T, Choi S-Y and Lee H 2012 *Angew. Chem., Int. Ed. Engl.* **51** 108
- [33] Seo S, Min M, Lee S M and Lee H 2013 *Nat. Commun.* **4** 1920
- [34] Kang J, Shin D, Bae S and Hong B H 2012 *Nanoscale* **4** 5527
- [35] Li X, Zhu Y, Cai W, Borysiak M, Han B, Chen D, Piner R D, Colombo L and Ruoff R S 2009 *Nano Lett.* **9** 4359
- [36] Reina A, Jia X, Ho J, Nezich D, Son H, Bulovic V, Dresselhaus M S and Kong J 2009 *Nano Lett.* **9** 30
- [37] Song H, Lee T, Choi N-J and Lee H 2007 *Appl. Phys. Lett.* **91** 253116
- [38] Kim Y et al 2012 *Nano Lett.* **12** 3736
- [39] Engelkes V B, Beebe J M and Frisbie C D 2004 *J. Am. Chem. Soc.* **126** 14287
- [40] Chu C, Na J-S and Parsons G N 2007 *J. Am. Chem. Soc.* **129** 2287
- [41] Wang G, Yoo H, Na S-I, Kim T-W, Cho B, Kim D-Y and Lee T 2009 *Thin Solid Films* **518** 824
- [42] Kim Y, Wang G, Choe M, Kim J, Lee S, Park S, Kim D-Y, Lee B H and Lee T 2011 *Org. Electron.* **12** 2144
- [43] Wang W Y, Lee T and Reed M A 2003 *Phys. Rev. B* **68** 035416
- [44] Wang W Y, Lee T and Reed M A 2005 *Rep. Prog. Phys.* **68** 523
- [45] Zhitenev N B, Erbe A and Bao Z 2004 *Phys. Rev. Lett.* **92** 186805
- [46] Bumm L A, Arnold J J, Dunbar T D, Allara D L and Weiss P S 1999 *J. Phys. Chem. B* **103** 8122
- [47] Fan F R F, Yang J P, Cai L T, Price D W, Dirk S M, Kosynkin D V, Yao Y X, Rawlett A M, Tour J M and Bard A J 2002 *J. Am. Chem. Soc.* **124** 5550
- [48] Holmlin R E, Haag R, Chabinyc M L, Ismagilov R F, Cohen A E, Terfort A, Rampi M A and Whitesides G M 2001 *J. Am. Chem. Soc.* **123** 5075
- [49] Kaun C C and Guo H 2003 *Nano Lett.* **3** 1521
- [50] Smalley J F, Feldberg S W, Chidsey C E D, Linford M R, Newton M D and Liu Y P 1995 *J. Phys. Chem.* **99** 13141
- [51] Wold D J, Haag R, Rampi M A and Frisbie C D 2002 *J. Phys. Chem. B* **106** 2813
- [52] Nijhuis C A, Reus W F and Whitesides G M 2009 *J. Am. Chem. Soc.* **131** 17814
- [53] Van Hal P A et al 2008 *Nat. Nanotechnology* **3** 749
- [54] Joachim C and Ratner M A 2005 *Proc. Natl. Acad. Sci. USA* **102** 8801
- [55] Venkataraman L, Klare J E, Tam I W, Nuckolls C, Hybertsen M S and Steigerwald M L 2006 *Nano Lett.* **6** 458
- [56] Krabbenborg S O, Wilbers J G E, Huskens J and van der Wiel W G 2013 *Adv. Funct. Mater.* **23** 770
- [57] Neuhausen A B, Hosseini A, Sulpizio J A, Chidsey C E D and Goldhaber-Gordon D 2012 *Acs Nano* **6** 9920
- [58] Wan A, Jiang L, Sangeeth C S S and Nijhuis C A 2014 *Adv. Funct. Mater.* **24** 4442
- [59] Nijhuis C A, Reus W F, Barber J R and Whitesides G M 2012 *J. Phys. Chem. C* **116** 14139
- [60] Li T et al 2012 *Adv. Mater.* **24** 1333
- [61] Li T et al 2013 *Adv. Mater.* **25** 4164
- [62] Salomon A, Boecking T, Seitz O, Markus T, Amy F, Chan C, Zhao W and Kahn A 2007 *Adv. Mater.* **19** 445
- [63] Xiang D, Jeong H, Lee T and Mayer D 2013 *Adv. Mater.* **25** 4845